



This is a repository copy of *Towards the implementation of an ion-exchange system for recovery of fluoride commodity chemicals. Kinetic and dynamic studies.*

White Rose Research Online URL for this paper:  
<https://eprints.whiterose.ac.uk/142786/>

Version: Accepted Version

---

**Article:**

Robshaw, T., Dawson, R. [orcid.org/0000-0003-4689-4428](https://orcid.org/0000-0003-4689-4428), Bonser, K. et al. (1 more author) (2019) Towards the implementation of an ion-exchange system for recovery of fluoride commodity chemicals. Kinetic and dynamic studies. Chemical Engineering Journal, 367. pp. 149-159. ISSN 1385-8947

<https://doi.org/10.1016/j.cej.2019.02.135>

---

Article available under the terms of the CC-BY-NC-ND licence  
(<https://creativecommons.org/licenses/by-nc-nd/4.0/>).

**Reuse**

This article is distributed under the terms of the Creative Commons Attribution-NonCommercial-NoDerivs (CC BY-NC-ND) licence. This licence only allows you to download this work and share it with others as long as you credit the authors, but you can't change the article in any way or use it commercially. More information and the full terms of the licence here: <https://creativecommons.org/licenses/>

**Takedown**

If you consider content in White Rose Research Online to be in breach of UK law, please notify us by emailing [eprints@whiterose.ac.uk](mailto:eprints@whiterose.ac.uk) including the URL of the record and the reason for the withdrawal request.



[eprints@whiterose.ac.uk](mailto:eprints@whiterose.ac.uk)  
<https://eprints.whiterose.ac.uk/>

## Accepted Manuscript

Towards the implementation of an ion-exchange system for recovery of fluoride commodity chemicals. Kinetic and dynamic studies

Thomas Robshaw, Robert Dawson, Keith Bonser, Mark D. Ogden

PII: S1385-8947(19)30374-2  
DOI: <https://doi.org/10.1016/j.cej.2019.02.135>  
Reference: CEJ 21048

To appear in: *Chemical Engineering Journal*

Received Date: 24 December 2018  
Revised Date: 16 February 2019  
Accepted Date: 19 February 2019

Please cite this article as: T. Robshaw, R. Dawson, K. Bonser, M.D. Ogden, Towards the implementation of an ion-exchange system for recovery of fluoride commodity chemicals. Kinetic and dynamic studies, *Chemical Engineering Journal* (2019), doi: <https://doi.org/10.1016/j.cej.2019.02.135>

This is a PDF file of an unedited manuscript that has been accepted for publication. As a service to our customers we are providing this early version of the manuscript. The manuscript will undergo copyediting, typesetting, and review of the resulting proof before it is published in its final form. Please note that during the production process errors may be discovered which could affect the content, and all legal disclaimers that apply to the journal pertain.



## Towards the implementation of an ion-exchange system for recovery of fluoride commodity chemicals. Kinetic and dynamic studies

Thomas Robshaw<sup>[a]\*</sup>, Robert Dawson<sup>[b]</sup>, Keith Bonser<sup>[c]</sup> and Mark D. Ogden<sup>[a]</sup>

\*Corresponding author address:

[a] Separations and Nuclear Chemical Engineering Research (SNUCER), Department of Chemical & Biological Engineering, University of Sheffield, Sheffield, S1 3JD, United Kingdom.

tjrobshaw1@sheffield.ac.uk

[b] Department of Chemistry, University of Sheffield, Sheffield, S3 7HF, United Kingdom.

[c] Bawtry Carbon International Ltd., Austerfield, Doncaster, DN10 6QT, United Kingdom.

### Keywords

Spent potlining, fluoride recovery, chelating resin, aluminium hydroxyfluorides, lanthanum, cryolite

### Abstract

*Spent potlining (SPL), a hazardous waste product from primary aluminium production, presents an important opportunity to recycle fluoride and conserve global fluorspar reserves. A novel strategy for treatment of the waste requires a selective fluoride-removal step from aqueous leachate. This has been demonstrated, using a Lanthanum-loaded chelating resin, in a series of kinetic and dynamic studies, with a view to industrial implementation. Kinetics could be described by the pseudo second-order model and uptake from SPL leachate was considerably higher than from equivalent NaF solutions, although observed rate constants were an order of magnitude less. Uptake of coexisting species and activation energy calculations*

*indicated that a novel complexation interaction between La centres and aqueous aluminium hydroxyfluorides dominated the uptake process. The resin operated efficiently in column studies, with a dynamic fluoride uptake capacity of 66.7 mg g<sup>-1</sup>, calculated by the Dose-Response model, which produced the best fit to the data. The attained elution profile suggested that fluoride recovery by cryolite precipitation would be feasible, which could be recycled back into primary aluminium production or exploited as a commodity. The resin was found to have high durability in performance studies over repeated batch treatments.*

## **1. Introduction**

Fluorspar ( $\text{CaF}_2$ ) is one of 27 critical raw materials, in terms of global supply-risk and economic importance [1]. It is the raw feedstock for the majority of industrial fluorochemicals, including the commercial polymers Teflon and Nafion [2]. Fluoride is also projected to be used in future generations of high power-density batteries [3]. Industrial recycling of fluoride is globally very limited, with fluoride-bearing waste streams generally viewed as nuisances to dispose of, rather than recycling opportunities [4-6].

The primary aluminium smelting industry creates ~1.3 million tonnes per year of spent potlining (SPL) waste. This is a hazardous material, comprising of “first-cut” (carbonaceous) and “second-cut” (cementitious) fractions. The former in particular, is a rich and untapped source of labile fluorides ( $\leq 18\%$ ) [7]. It is particularly desirable to recycle the fluoride content of SPL, since the Hall-Hèroult electrolysis process for alumina reduction consumes  $\leq 50$  kg  $\text{AlF}_3$  per tonne of metallic aluminium produced [8]. The main component of the Hall-Hèroult electrolysis bath is cryolite ( $\text{Na}_3\text{AlF}_6$ ), which is increasingly a by-product of modern Al smelters, rather than consumed as a raw material [9]. It is nonetheless a valuable commodity chemical and still purchased in large quantities by the industry globally [10]. The market prices for  $\text{AlF}_3$  and cryolite, which are both produced from fluorspar, are on global long-term upwards trends, due to continued high demand and inefficient fluorine recycling [11]. Most current industrial methods for SPL treatment are pyrometallurgical and focus on its conversion to an environmentally benign form via calcination or vitrification, hence not recycling a large fraction of the trapped fluorides [12-14].

Hydrometallurgical treatment systems are rare, with the low caustic leaching and lime (LCLL) process used by Rio Tinto Alcan being the only industrial example [15]. It is however known that first-cut SPL may be almost completely cleansed of its fluoride content via a simple two-step leach, using NaOH, then H<sub>2</sub>SO<sub>4</sub> solutions [16, 17]. These two leachate streams may then be combined, producing a liquor of high aqueous fluoride concentration and also containing many co-existing anions and complexing metal cations.

Our current work focusses on implementing an ion-exchange system to selectively remove the fluoride from this multi-component leachate, consisting of sorbent-filled columns, through which the leachate is pumped. We chose to investigate metal-loaded cation resins for this purpose, since these materials are easily modified, have been optimised for column-based systems, are economical and have good potential for regeneration [18-20]. Several studies have also used the more economical lanthanides (La and Ce) for sorbent modification for fluoride selectivity. Modified materials include ion-exchange resins [21], alumina [22, 23] and chitosan [24, 25]. However, the aqueous systems studied generally had low fluoride concentration ranges and either low or uncertain ionic strength and appeared to be conducted with polishing or detoxifying applications in mind. Meenakshi and Viswanathan studied the performance of commercial ion-exchange resins over a fluoride concentration range of 2 – 10 mg L<sup>-1</sup> and conducted a field trial on a water source of ~500 mg L<sup>-1</sup> total dissolved solids [26]. Wassay *et al.* observed the performance of a lanthanide-modified alumina in the removal of fluoride from semiconductor production wastewater, in which the most concentrated co-anion was NO<sub>3</sub><sup>-</sup> at ~390 mg L<sup>-1</sup> [23]. Oke *et al.* showed the industrial implementation of an Al-loaded ion-exchange resin

column for treatment of an aqueous waste stream from a chemicals manufacturer. However, the system was downstream of an independent precipitation unit, which greatly reduced the inlet fluoride concentration [18]. Further examples of the aqueous systems studied are seen in the Supporting Information, Table S1. None of the studies cited produced an elution profile to investigate how the adsorbed fluoride might be removed from a column in a purer form, to allow its recovery. We were unable to find any documentation of fluoride removal, by ion-exchange, from waste streams of high  $[Al^{3+}]$ , which profoundly changes the chemistry of the solution, due to its high fluoride affinity [27].

To extract the fluoride from SPL leachate, we chose an aminophosphonic acid resin, Purolite MTS9501, loaded with  $La^{3+}$  ions, hypothesising that the chelating functionality would be a sufficiently strong interaction to allow the resin to perform in the challenging conditions of aqueous SPL leachate, with minimal  $La^{3+}$  leaching. Initial isotherm studies in fact suggested that the resin was effective even in highly concentrated liquor ( $[F^-] \leq 1500 \text{ mg L}^{-1}$ ), producing a maximum uptake capacity of  $>120 \text{ mg g}^{-1}$  (calculated by Langmuir isotherm). This was significantly greater than previous published data for metal-loaded resins [19, 28, 29], although smaller than the figure for uptake from NaF solution alone, which was  $187 \text{ mg g}^{-1}$ . The results appeared to be due to a combination of the expected  $La^{3+}$  ligand-exchange functionality and unexpected precipitation of amorphous aluminium hydroxyfluoride (AHF) complexes within the resin macropores [30]. The unusual co-uptake of fluoride and aluminium led to the hypothesis that cryolite or  $AlF_3$  recovery could be possible through known technology [16, 27, 31]. This would significantly reduce the demand by the aluminium industry for geological fluorspar. Uptake from simple NaF solutions

alone also produced unexpected phenomena, as fluoride was taken up not only by ligand-exchange, but also  $\text{LaF}_3$  and  $\text{NaF}$  precipitation. The heterogeneity of the postulated adsorption mechanisms is shown in Fig. 1.

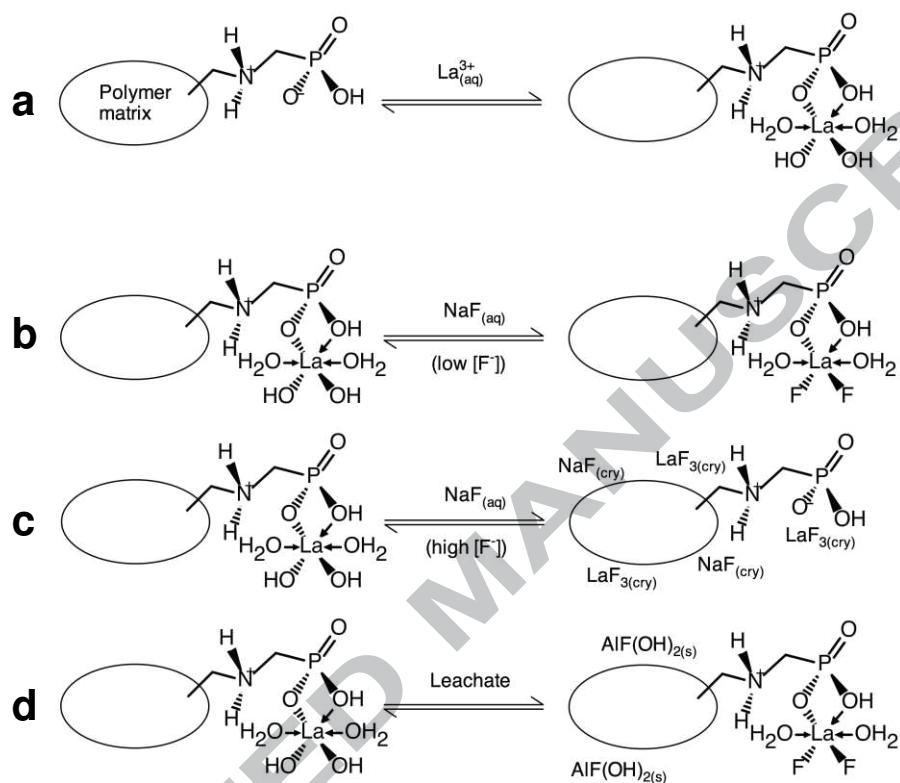


**Fig. 1.** Previously proposed mechanisms of fluoride uptake onto La-MTS9501 resin [30]. (a) = pre-loading of MTS9501 with  $\text{La}^{3+}$ . (b) = contact with dilute  $\text{NaF}$  solutions, showing the known ligand-exchange process. (c) = contact with concentrated  $\text{NaF}$  solutions, showing  $\text{LaF}_3$  crystallisation and  $\text{NaF}$  salt precipitation. (d) = contact with leachate, showing ligand-exchange and precipitation processes. “cry” = crystalline.

However, to assess La-MTS9501 resin for its intended purpose requires understanding of the kinetic behaviour of the system, specifically with respect to the effects of temperature and concentration, and particularly, given the unusual uptake mechanism proposed. Performance in dynamic operations is also crucial, including breakthrough behaviour and the fluoride and aluminium elution profiles which may be attained. We therefore report here on the kinetic and dynamic behaviour of fluoride uptake via La-MTS9501 treatment with a SPL simulant leachate stream, including, for the first time, a calculation of the activation energy for fluoride uptake

by a metal-loaded ion-exchange resin. The focus of the research remains on the performance of La-MTS9501 when contacted with undiluted leachate of high ionic strength. We hope, in this way to continue to establish fundamental understanding of the nature of fluoride uptake in solutions of high  $\text{Al}^{3+}$  concentration, which has not previously been reported. We also aim to understand, from elution data, which commodity chemicals may be feasibly recovered via the proposed hydrometallurgical process, which again is yet unreported.

Similarly to our previous work, uptake behaviour from analytical NaF solutions and at higher dilutions are also presented, for better understanding of uptake mechanisms, valid comparison to the literature and other potential fluoride recycling routes.

## 2. Experimental

### 2.1. Materials and reagents

A liquor was prepared, to simulate the leachate produced by contact of first-cut SPL with dilute NaOH, followed by dilute  $\text{H}_2\text{SO}_4$ , as per the LCLL process [15]. In addition to high concentrations of  $\text{Na}^+$  and  $\text{SO}_4^{2-}$ , the liquor contained  $1500 \text{ mg L}^{-1}$  fluoride and

1200 mg L<sup>-1</sup> Al<sup>3+</sup>. Synthesis and concentrations of co-ions are given in the Supporting Information, Table S2. Aqueous speciation was determined using the Aqion software package v6.4.7. [32]. See the Supporting Information, p3 for inputted parameters and results. Concentrations were derived from characterisation of first-cut SPL material by previous studies and assuming ~100% leaching of contaminants was possible [7, 33, 34]. For comparative work, NaF solutions were made up by dissolving the required amount of NaF salt in deionised water. Puromet™ MTS9501 resin was kindly donated by Purolite. Physical parameters are found in the Supporting Information, Table S5. The resin was converted to its protonated form by batch treatment of ~25 g resin (wet mass) with 1 L of 1 M HCl, then loaded with La<sup>3+</sup> ions by batch treatment of the same with 1 L of 10 g L<sup>-1</sup> La<sup>3+</sup> solution, made by dissolving LaCl<sub>3</sub>·7H<sub>2</sub>O in deionised water. As previously established, this resulted in a maximal La-loading of 256 mg g<sup>-1</sup> (1.84 mmol g<sup>-1</sup>) [30]. The La-MTS9501 resin was washed with 5 x 200 bed volumes (BVs) of deionised water (bed volume = equivalent water volume to that of a given resin mass) and dried for 24 h in an air-flow oven at 50°C. Relevant parameters for the modified resin, from equilibrium studies, are found in the Supporting Information, Table S6.

## 2.2. Solid-state analysis of resin

Samples of MTS9501 resin at various process stages were first washed with 10 x 200 BVs of deionised water, then ground to a fine slurry, using a mortar and pestle, then dried in an air-flow oven at 50°C for a minimum of 24 h. X-ray diffraction (XRD) analysis was performed using a Bruker D2 Phaser X-ray diffractometer.

Thermogravimetric analysis (TGA) was conducted using a Perkin Elmer Pyris1.

Further details are in the Supporting Information, p6.

### 2.3. Static kinetic experiments

Kinetic data was acquired for fluoride removal from the leachate at dilutions of 1/100 ( $[F^-] \approx 15 \text{ mg L}^{-1}$ ), 1/30 ( $[F^-] \approx 50 \text{ mg L}^{-1}$ ), 1/10 ( $[F^-] \approx 150 \text{ mg L}^{-1}$ ), 1/3 ( $[F^-] \approx 500 \text{ mg L}^{-1}$ ) and as-prepared ( $[F^-] \approx 1500 \text{ mg L}^{-1}$ ). Data was similarly acquired from NaF solutions of equivalent  $[F^-]$ . An additional experiment was performed at  $[F^-] \approx 5000 \text{ mg L}^{-1}$ , to examine a system dominated by NaF precipitation over ligand-exchange processes and its effect on kinetic parameters.

In kinetic experiments, a 1 L Nalgene<sup>®</sup> bottle, containing 500 mL of NaF solution or simulant leachate and a large magnetic stirrer, was held, via a clamp, in a 2 L polypropylene beaker, containing tap water and also fitted with a large magnetic stirrer. This was placed on a combined stirrer/hotplate and heated to the desired temperature or cooled with ice. A thermometer was used to ensure the temperature of the bath did not fluctuate by  $>1^\circ\text{C}$ . 5.0 g La-MTS9501 (dry mass) was placed in the fluoride-bearing solutions and left to stir for up to 72 h. At predetermined time periods, 50  $\mu\text{L}$  aliquots were removed from the bottle. The total volume removed from the bottle did not exceed 5.0 mL and the lid was closed between samplings. Most experiments were conducted at  $20^\circ\text{C}$ , the range being 2 -  $43^\circ\text{C}$ . The pH of experimental solutions was not adjusted.

The aliquots were diluted by a factor of  $\geq 100$  and their fluoride concentration was analysed using a Sciquip fluoride ion-selective electrode (ISE). Each sample also

contained 50% ionic strength adjustment buffer (Supporting Information p5). The Al, and Ca concentration of a number of leachate samples (without added buffer) was determined, using a Thermo Scientific iCAP 6000 ICP-OES. The concentrations of co-existing anions  $\text{Cl}^-$ ,  $\text{NO}_3^-$  and  $\text{SO}_4^{2-}$  were quantified using a Metrohm 883 Basic IC plus ion chromatography (IC) system (Supporting Information, p5).

#### 2.4. Dynamic experiments

Breakthrough curves for the two matrices were attained for an inlet fluoride concentration of 15 and 1500  $\text{mg L}^{-1}$ . 2.0 g La-MTS9501 (dry mass) was placed inside a 10 mL polypropylene syringe, fitted with two porous frits, both above and below the resin bed. This was connected to a Watson Marlow 120U peristaltic pump using Watson Marlow Marprene<sup>®</sup> tubing of 0.8 mm internal diameter, which pumped NaF solution or simulant leachate through the column in a reverse-flow system. The eluent was fed to an automated fraction-collector (Bio Rad, model 2110), which was set to collect fractions of 0.5 BVs (3 mL). The pump was previously calibrated over a period of one day to give a linear flow rate of one BV (6 mL) per h. Fractions were diluted by a factor  $\geq 10$  and were analysed by ISE, ICP-OES and IC as previously described.

In elution experiments, a similar dry mass of La-MTS9501, fully-loaded with fluoride or mixed leachate contaminants via the breakthrough technique, was set up as previously described. Loaded species were eluted using the same flow rate as for breakthrough experiments. Eluent used, in order, were deionised water, 0.01 M NaOH, 1 M NaOH and 3 M HCl. Concentrations of fluoride and co-anions were

determined by IC, as previously described. Concentrations of Al and Ca were determined by ICP-OES, also as previously stated.

## 2.5. Investigation of uptake behaviour by fitting to kinetic models

The uptake of fluoride and co-contaminants in the leachate at various time intervals was determined via equation (1):

$$q_t = (C_i - C_t) \times V/W \quad (1)$$

where  $q_t$  is the fluoride uptake capacity of the resin at a given time,  $C_i$  is the initial fluoride concentration of the solution in  $\text{mg L}^{-1}$ ,  $C_t$  is the fluoride concentration of the solution at equilibrium in  $\text{mg L}^{-1}$  at a given time,  $V$  is the volume of solution contacted in L and  $W$  is the dry mass of resin used in g. Fluoride ligand-exchange uptake data has previously been proposed to obey well both pseudo first-order and pseudo second-order kinetics [23, 25]. Therefore we chose to fit the data to the commonly used Lagergren pseudo first-order (PFO) [35] and Blanchard pseudo second-order (PSO) [36] rate equations (2 & 3):

$$q_t = q_e(1 - e^{-k_1 t}) \quad (2)$$

$$q_t = \frac{k_2 q_e^2 t}{1 + k_2 q_e t} \quad (3)$$

where  $q_e$  is the uptake capacity at equilibrium,  $t$  is time in minutes and  $k_1$  and  $k_2$  are the pseudo first- and second-order rate constants in  $\text{min}^{-1}$  and  $\text{g mg}^{-1} \text{min}^{-1}$ . Model-fitting was achieved using the Microsoft Excel SOLVER add-in (GRG nonlinear engine) [34]. Additional parameters, derived from PFO and PSO equations, were calculated using equations (4 & 5):

$$t_{1/2} = \frac{1}{k_n q_e} \quad (4)$$

$$h_0 = k_2 q_e^2 \quad (5)$$

where  $n = 1$  or  $2$ , corresponding to PFO or PSO equations,  $t_{1/2}$  is the sorption half-time (min) and  $h_0$  is the initial sorption rate ( $\text{mg g}^{-1} \text{min}^{-1}$ ) All other parameters are as previously described. The  $k$  values attained from experiments at different temperatures were used to create Arrhenius plots, using equation (6):

$$k = A e^{\frac{-E_a}{RT}} \quad (6)$$

Where  $A$  is the pre-exponential factor,  $E_a$  is the activation energy for the process ( $\text{J mol}^{-1}$ ),  $R$  is the gas constant ( $8.314 \text{ J K}^{-1} \text{ mol}^{-1}$ ) and  $T$  is the experimental temperature (K).

At high fluoride concentrations in particular, such uptake systems are influenced by diffusion processes, as the concentration gradient increasingly dominates the behaviour [35]. We therefore checked agreement of data to the Boyd film-diffusion model [37], shown in equation (7)

$$\ln(1 - F) = k_{fd}t \quad (7)$$

where  $F$  is the fractional attainment of equilibrium at time  $t$  and  $k_{fd}$  is the film-diffusion rate constant ( $\text{min}^{-1}$ ). Therefore, in a plot of  $-\ln(1 - C_t/C_i)$  vs  $t$ , a linear gradient would indicate that the uptake rate is controlled by the movement of adsorbate ions within the pores of the resin beads (intraparticle-diffusion). A non-linear gradient would suggest the rate is controlled by the movement of the adsorbate through the hydrous film layer surrounding the adsorbent particles (film-diffusion), or the chemical reaction at the surface [37, 38]. We also determined the agreement of the data with the intraparticle diffusion model [39], seen in equation (8):

$$q_t = k_{id}t^{1/2} + C \quad (8)$$

where  $k_{id}$  is the intraparticle-diffusion rate constant ( $\text{mg g}^{-1} \text{min}^{-1/2}$ ) and  $C$  is a constant relating to the thickness of the adsorbent film layer. Data plots of  $q_t$  vs  $t^{1/2}$  were

produced. It is accepted that, if such a plot has a linear gradient and passes through the origin, the adsorption is entirely controlled by intraparticle-diffusion [40, 41]. We finally studied the adherence of the uptake to the Elovich model [42], applying the Chien and Clayton simplification [43], which has frequently been applied to chemisorption-dominated systems [41]. This is shown in equation (9):

$$q_t = \frac{1}{\beta} \ln(t) + \frac{1}{\beta} \ln(\alpha\beta) \quad (9)$$

where  $\alpha$  is the initial rate constant ( $\text{mg g}^{-1} \text{min}^{-1}$ ) and  $\beta$  is a desorption constant ( $\text{mg g}^{-1}$ ). Hence, if a plot of  $q_t$  vs  $\ln(t)$  produces a linear gradient, the system may be described by the Elovich equation. This is often interpreted to mean that adsorption involves two or three simultaneous first-order reactions [43].

Closeness of fit with these three models was estimated via linear regression, to derive  $R^2$  values.

## 2.6. Investigation of uptake behaviour by fitting to dynamic models

The breakthrough data were fitted to a number of commonly applied models, again using SOLVER and non-linear regression. The relevant equations for each model and full experimental dataset are found in the Supporting information, p23. For brevity, only the Dose-Response model [44], which, as shall be seen, provided the best description of fluoride breakthrough, is presented in the main text. The Dose-Response model is shown in Equations (10 & 11).

$$\frac{c}{c_i} = 1 - \frac{1}{1 + \left(\frac{V_{\text{eff}}}{b}\right)^a} \quad (10)$$

$$q_0 = \frac{bc_i}{m} \quad (11)$$

In these equations  $V_{ef}$  is the volume of solution eluted from the column (mL),  $a$  and  $b$  are constants of the Dose-Response model,  $q_0$  is the theoretical maximum uptake capacity of the resin in a dynamic environment ( $\text{mg g}^{-1}$ ) and  $m$  is the dry mass of resin (g).

From elution data, the total masses of fluoride, Al and Ca eluted were found by calculating the area underneath the respective elution profiles and comparing to the total mass of each species loaded on to the column. This in turn was calculated from the Dose-Response model  $q_0$  values attained, allowing an approximate % recovery to be derived.

## 2.7. Batch fluoride extraction experiments and resin regeneration attempts

Additional batch experiments were carried out, at ambient temperature, to corroborate kinetic and dynamic data. In certain experiments the initial  $[\text{Al}^{3+}]$  was altered, by controlling the addition of  $\text{Al}_2(\text{SO}_4)_3$  in the synthetic leachate, with all other factors being kept constant.

In a typical procedure, ~100 mg of La-MTS9501 (dry mass) was contacted with 25 mL solution of known fluoride concentration in a 50 mL polypropylene screw-top tube. This was sealed and placed on the orbital shaker at 100 rpm for 24 h. Solutions were analysed via ISE, as previously described. The equilibrium uptake capacity of the resin ( $q_e$ ) in  $\text{mg g}^{-1}$  was estimated using equation (12):

$$q_e = (C_i - C_e) \times V/W \quad (12)$$

where  $C_e$  is the fluoride concentration of the solution at equilibrium in  $\text{mg L}^{-1}$  and all other terms as per equation (1).

The resin was regenerated by batch treatment of ~25 g resin (wet mass) with 1 L 0.01 M NaOH solution. Contact time was 1.0 h. The regenerated resin was washed 5 times with 200 bed volumes of deionised water and dried for 24 h in an air-flow oven at 50°C before being reused. The approximate maximum uptake capacity of the resin by batch treatment with as-prepared simulant leachate ( $[\text{F}] \approx 1500 \text{ mg L}^{-1}$ ) was determined over five cycles of regeneration. At the end of the five cycles, the resin was further contacted, using the same technique, with 3 M HCl, returning it to the protonated form. It was then re-loaded with  $\text{La}^{3+}$  as previously described, and uptake capacity was again determined. Analysis was performed in triplicate and results averaged.

### 3. Results and Discussion

#### 3.1. Investigation of uptake kinetics from media at various concentrations

In the case of the as-prepared liquor, Al kinetic data was acquired to attempt to further understanding of the uptake mechanism of the system. Ca data was acquired for comparison, as previous work had revealed that it was taken up in small amounts ( $<0.5 \text{ mg g}^{-1}$ ) in thermodynamic studies [30], yet was not believed to play a role in the fluoride uptake mechanism.

For fluoride uptake, both from leachate and NaF solutions, the full range of  $R^2$  values from linear data plots previously described, for film-diffusion, intraparticle-diffusion and Elovich models are shown in the Supporting Information, Table S7. The two diffusion-controlled model plots produced curved gradients for all fluoride uptake experiments. The average  $R^2$  values attained for film-diffusion plots were 0.295 (leachate) and 0.336 (NaF solutions), indicating that film-diffusion and/or chemical reaction were influential to the rate of adsorption [38]. For intraparticle-diffusion plots, the  $R^2$  values were 0.723 (leachate) and 0.620 (NaF solutions). This suggests that, under these experimental conditions, the intraparticle-diffusion step was not rate-limiting for the fluoride transfer on to the resin over the experimental timeframe. Similar data have been observed previously for uptake of rare earth metal ions by macroporous resins [45], which is unsurprising, as a macroporous internal structure should ensure rapid transport of the adsorbate to binding sites. The plot of  $q_t$  vs  $t^{1/2}$  yielded a curve in many cases (Supporting Information, Fig S8b and S16b). This has been proposed to indicate that boundary-layer diffusion, intraparticle diffusion and chemical reaction dominated at different uptake stages [46, 47]. There was no indication of the rate-determining step changing from film- to intraparticle-diffusion at higher fluoride  $C_i$ , as was originally shown by Boyd *et al.* [37].

The Elovich model, gave a reasonable description of the data in many cases, but for other experiments was not sufficient. The average  $R^2$  value for leachate experiments was 0.911 (range = 0.852 – 0.995), and for NaF solution experiments was 0.826 (range = 0.669 – 0.958). A strongly linear gradient was observed specifically in the plot of  $q_t$  vs  $\ln(t)$  in leachate experiments at high dilutions over some, or all of the experimental timeframe (Supporting Information, Fig. S4c and S6c). Elovich plots that

exhibit sections of linearity, as is the case here, have been proposed to describe heterogeneous adsorption processes [40, 45], which agrees with existing knowledge of this system.

Calculated parameters from fitting of the same data to the PFO model and the full range of associated  $R^2$  values are also presented in the Supporting Information, Table S8. The average  $R^2$  value for leachate experiments was 0.897 (range = 0.828 – 0.960), and for NaF solution experiments was 0.842 (range = 0.785 – 0.899). The PSO model gave a superior description of the adsorption for nearly all experiments and associated parameters were therefore considered more valid and are shown in Table 1.

**Table 1.** SOLVER fitting of fluoride uptake kinetic data to PSO model. Uptake shown from leachate and NaF solutions of various concentrations. Resin dry mass = 5.0 g, initial solution volume = 500 mL,  $T = 20^\circ\text{C}$ .

Sample	$q_e$ ( $\text{mg g}^{-1}$ )	$k_2$ ( $\text{min}^{-1}$ )	$t_{1/2}$ (min)	$h_0$	$R^2$
Leachate 1/100 dilution	$0.729 \pm 0.012$	$6.07 \pm 0.77 \times 10^{-2}$	$22.6 \pm 5.8$	$3.23 \pm 0.82 \times 10^{-2}$	0.945
Leachate 1/30 dilution	$3.78 \pm 0.14$	$3.14 \pm 0.492 \times 10^{-2}$	$8.53 \pm 2.72$	$0.355 \pm 0.125$	0.930
Leachate 1/10 dilution	$7.17 \pm 0.89$	$7.28 \pm 0.96 \times 10^{-2}$	$21.1 \pm 3.5$	$0.443 \pm 0.142$	0.968
Leachate 1/3 dilution	$16.4 \pm 0.2$	$1.88 \pm 0.08 \times 10^{-3}$	$32.6 \pm 2.7$	$0.501 \pm 0.042$	0.993
Leachate as-prepared	$26.4 \pm 0.4$	$4.73 \pm 0.73 \times 10^{-3}$	$24.6 \pm 4.0$	$3.3 \pm 1.0$	0.929
Leachate as-prepared (Al)	$21.6 \pm 0.30$	$1.62 \pm 0.19 \times 10^{-3}$	$28.6 \pm 3.4$	$0.756 \pm 0.090$	0.937
Leachate as-prepared (Ca)	$1.88 \pm 0.02$	$4.65 \pm 0.75 \times 10^{-2}$	$11.5 \pm 1.8$	$0.164 \pm 0.026$	0.833
NaF solution $C_i \approx 15 \text{ mg L}^{-1}$	$0.615 \pm 0.007$	$0.546 \pm 0.082$	$2.98 \pm 0.45$	$0.206 \pm 0.031$	0.951
NaF solution $C_i \approx 50 \text{ mg L}^{-1}$	$1.68 \pm 0.04$	$0.499 \pm 0.019$	$2.93 \pm 0.99$	$0.390 \pm 0.044$	0.862
NaF solution $C_i \approx 150 \text{ mg L}^{-1}$	$3.44 \pm 0.03$	$0.167 \pm 0.012$	$6.68 \pm 1.02$	$2.07 \pm 0.06$	0.944
NaF solution	$5.07 \pm 0.13$	$0.110 \pm 0.031$	$1.80 \pm 0.52$	$2.82 \pm 0.81$	0.877

$C_i \approx 500 \text{ mg L}^{-1}$					
NaF solution	$14.0 \pm 0.8$	$2.10 \pm 0.83 \times 10^{-2}$	$3.40 \pm 1.36$	$4.12 \pm 1.66$	0.751
$C_i \approx 1500 \text{ mg L}^{-1}$					
NaF solution	$135 \pm 3$	$1.62 \pm 0.50 \times 10^{-3}$	$4.58 \pm 1.41$	$29.5 \pm 4.57$	0.897
$C_i \approx 5000 \text{ mg L}^{-1}$					
For F uptake, average $R^2$ value for leachate experiments was 0.953 and for NaF solution experiments was 0.880.					

Kinetic data for fluoride, Al and Ca uptake from the undiluted leachate are shown in Fig. 2. The corresponding data for NaF solution uptake, where fluoride  $C_i = 1500 \text{ mg L}^{-1}$ , is also shown. Data are presented with fitting to the PSO model. Leaching of La was also checked in these experiments and was observed to reach a maximum of  $\sim 20 \text{ mg L}^{-1}$  in the leachate medium. Leached La concentration was below detectable limits for the NaF solution medium. The full dataset in graphical form may be seen in the Supporting Information, p6

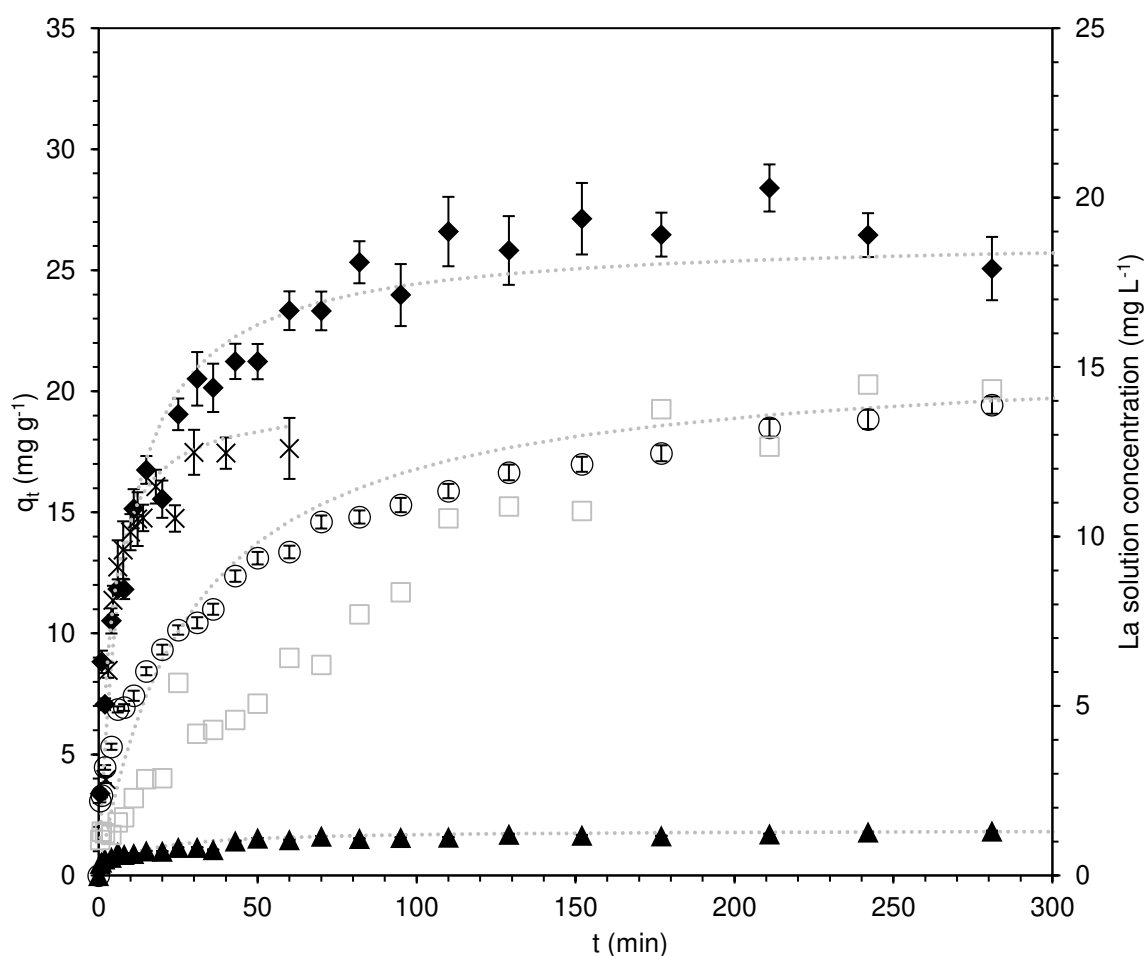


**Fig. 2.** Uptake of fluoride, Al and Ca from as-prepared simulant leachate and NaF solution (fluoride  $C_i = 1500 \text{ mg L}^{-1}$ ) by La-MTS9501 over time, with data fitted to pseudo second-order kinetic model, represented by dotted lines. Includes La-leaching from the resin. Resin dry mass = 5.0 g. Initial solution volume = 500 mL.  $T = 20^\circ\text{C}$ .  $\blacklozenge$  = fluoride from leachate.  $\circ$  = Al from leachate.  $\blacktriangle$  = Ca from leachate.  $\square$  = La loss into leachate (right-hand y axis).  $\times$  = fluoride from NaF solution. In some cases, error bars are too small to be seen.

The reasonable adherence of the fluoride uptake behaviour to PSO kinetics is consistent with an observation by Viswanathan & Meenakshi for similar resins [19] and for many other studies which have used rare earth functionality within other support matrices (Supporting Information, Table S1). Further studies have cited the PFO model as suitable for describing fluoride adsorption by ion-exchange resins [48, 49], but as the two models were not directly compared in these cases, it is difficult to conclude whether La-MTS9501 behaves typically or atypically for a metal-loaded

resin. In our work, the generally poorer agreement with the PFO model suggested a chemisorption mechanism dominated over all concentrations tested [50]. It should be noted that we do not propose this based solely on kinetic data, but also on previous X-ray photoelectron spectra, which indicated clear changes to the La bonding environments upon resin-contact with both leachate and NaF solutions [30]. An exception in the data is the case of uptake from NaF solution where  $[F^-] \approx 5000 \text{ mg L}^{-1}$ . This is consistent with our previous results, which suggested that the dominant uptake mechanism from NaF solution changed from chemisorption to physisorption (crystalline NaF precipitation) at very high  $[F^-]$ .

The attained  $q_e$  values via kinetic experiments are much higher for leachate experiments than NaF solution experiments. This is in contrast to the prior equilibrium study, in which our  $q_{\text{max}}$  values, determined by Langmuir isotherm-fitting, were higher for the NaF solution [49]. The disparity is likely due to the increased resin:solution ratio in kinetic experiments and results suggested that the practical operating capacity for La-MTS9501 might be considerably higher, when applied to aluminium industry leachate, rather than a simpler matrix. Interestingly, a slight “double plateau” was observed in some NaF solution kinetic data plots (Supporting Information, Figs. S12 & S15). It is possible that this represents the point where the first  $\text{OH}^-/\text{F}^-$  ligand-exchange is complete on the majority of La centres, since the second exchange is thermodynamically less-favoured and would therefore be slower [49]. This phenomenon has been observed in previous studies, where complexing metals have been used as active sites for fluoride ligand-exchange [48, 51, 52], but does not appear to have been commented on. The behaviour was not observed in all NaF uptake experiments. No double plateau was observed in any leachate uptake

experiments, suggesting that the adsorption mechanism did not involve ligand-exchange.

For uptake from NaF solution, the calculated rate constants were considerably higher than previously reported for metal-loaded resins at comparable  $C_i$  values [53, 54] and for other rare-earth-functionalised sorbents [22, 24]. This may be partially attributed to the large accessible surface area of the macroporous resin. In support of this, the moisture-content range of MTS9501 (60-68%) is greater than that of commercial equivalent Lewatit® TP260 (58-62%) [55, 56]. The kinetics of uptake from leachate were generally slower by an order of magnitude. This would be expected, given the higher ionic strength of the leachate, as previously stated, which is known to retard adsorption kinetics [57]. As-prepared leachate ionic strength was calculated by Aqion to be  $24.8 \text{ mmol L}^{-1}$ , compared to  $6.23 \text{ mmol L}^{-1}$  for the NaF solution of equivalent fluoride concentration [32].

The dependence of  $k_2$  values on fluoride  $C_i$  for the 2 aqueous systems was examined and is shown in Fig 3. The relationship of  $k_2$  with  $h_0$  values is shown in the Supporting Information, Fig. S23.

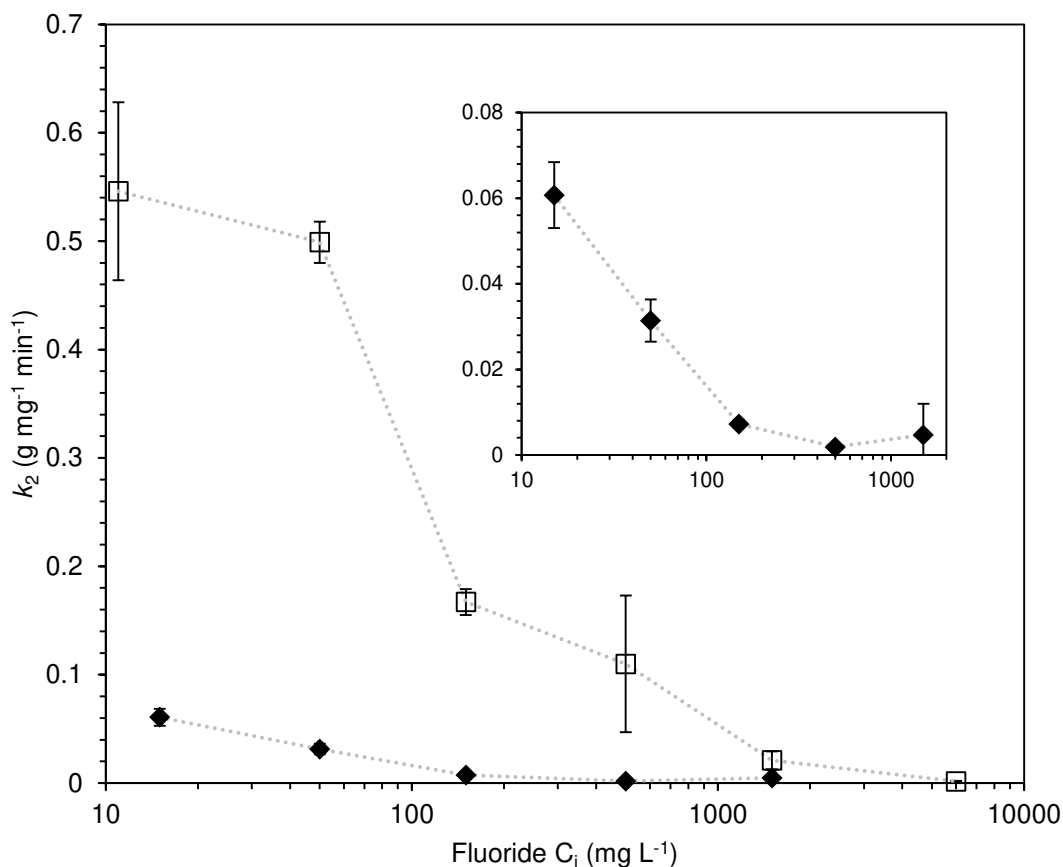


**Fig. 3.** Relationship between fluoride  $C_i$  and observed  $k_2$  value for uptake from leachate (◆) and NaF solution (□). x axis is logarithmic for clarity. Enlargement shows change in gradient for leachate matrix.

Fig. 3 shows that the effect of increasing  $C_i$  on the  $k_2$  values was not equivalent for the 2 matrices. Interestingly, with uptake from leachate, the  $k_2$  value appears to be dependent on the  $\log_{10}$  of  $C_i$  across the low end of the concentration range, whereas there is minimal correlation for NaF solution uptake. This may be because uptake from NaF solution is dominated by different processes across the  $C_i$  range, including ligand-exchange,  $\text{LaF}_3$  crystallisation and precipitation [58] and NaF physisorption and crystallisation [28, 30], whereas AHF uptake from leachate is a more homogenous process. It has been shown that  $k_2$  values are not accurately predicted from  $C_i$  values across a wide concentration range [59]. Contrary to our findings, Lv *et al.* studied the effect of changing  $C_i$  upon the uptake of fluoride by layered double hydroxide sorbent and reported that  $k_2$  values broadly increased with an increase in

$C_i$ , although again, no linear trend was observed [46]. Viswanathan and Meenakshi found no overall trend in the relationship between  $C_i$  and  $k_2$  for fluoride uptake by an alumina-chitosan complex, using a  $C_i$  range of 9 – 15 mg L<sup>-1</sup> [60]. It can also be observed (Table 1) that there is no correlation between fluoride  $C_i$  and calculated  $t_{1/2}$  values. Interestingly however, the values attained for the as-prepared leachate and 1/100 dilution leachate experiments were almost equivalent. This suggested that operating at lower dilutions may indeed be practical industrially, from the point of view of rapid and efficient column-loading.

The co-uptake of metal ions data (Fig. 2) demonstrated that Al and fluoride appeared to be taken up synergistically, or at least in conjunction until the ~200 min stage. This was contrary to expectations, as it was thought that a OH<sup>-</sup>/F<sup>-</sup> ligand-exchange process would dominate in the first few minutes of adsorption, with negligible Al uptake. This prompted us to examine the molar ratio of the two adsorbed species over time (Supporting Information, Fig. S31). This revealed that apart from a brief period at ~1 min, the F<sup>-</sup>:Al<sup>3+</sup> molar ratio remains at ~2.5:1 until ~100 min, then drops gradually to ~1.5:1. This suggests that the dominant mechanism throughout the uptake process is the adsorption of aqueous AHFs. Aqion calculations are in good agreement with this theory (Supporting Information, Table S3), since the most prevalent species in solution are AlF<sub>3</sub> and AlF<sub>2</sub><sup>+</sup>, hence the ~2.5:1 molar ratio initially observed is sensible. Over time, a slow equilibrium process on the resin surface between 100 and 700 min appears to release some fluoride back into solution at the same time as further AHF adsorption, meaning the ratio tends towards 1:1. This is, in fact, consistent with previous XPS data [30], which indicated that the dominant AHF species on the resin surface, after equilibrium had been reached, was closely related

to  $\text{AlF}(\text{OH})_2$ , rather than more fluoride-rich species. The uptake of Ca was seemingly independent of both fluoride and Al, as its  $k_2$  value was an order of magnitude higher. It is possible that  $\text{Ca}^{2+}$  ions occupied the more hindered aminophosphonic acid coordination sites, which the  $\text{La}^{3+}$  ions were not sterically able to reach. The leaching of La into the solution is too minor to be correlated to the uptake of Al or Ca and is likely a cumulative effect of the high ionic strength liquor.

### 3.2. Determination of activation energy for the two systems

The full dataset for temperature-varied experiments, in graphical form, is shown in the Supporting Information, p18, including parameters calculated from the PSO rate equation. Increasing the temperature of the system increased the rate of fluoride uptake, but resulted in lower  $q_e$  values. The effect on  $q_e$  was however much less pronounced for uptake from the leachate than for uptake from NaF solutions (Supporting Information, Table S9). This infers that the uptake of free fluoride on to the resin was a more exothermic process than AHF complexation ( $\Delta H_f$  for  $\text{LaF}_3 = -1732 \text{ kJ mol}^{-1}$ ). Viswanathan and Meenakshi observed that  $q_e$  values for fluoride uptake by metal-loaded cation-exchange resins similarly decreased with increasing temperature [61].

The  $k_2$  values were subsequently used to produce Arrhenius plots (Supporting Information, Fig. S30). The extracted parameters for the leachate and NaF solution matrices are displayed in Table 2.

**Table 2.** Arrhenius parameters calculated for the two systems. Fluoride  $C_i = 150 \text{ mg L}^{-1}$ . Resin dry mass = 5.0 g. Initial solution volume = 500 mL.  $T = 2\text{-}43^\circ\text{C}$ .

Matrix	$E_a$ (kJ mol <sup>-1</sup> )	A	R <sup>2</sup>
--------	-------------------------------	---	----------------

Leachate	$34.6 \pm 4.3$	$1.42 \pm 0.13 \times 10^8$	0.970
NaF solution	$62.6 \pm 0.71$	$2.66 \pm 0.23 \times 10^{14}$	0.975

Experiments to determine  $E_a$  values for the two systems were performed at  $C_i \approx 150$  mg L<sup>-1</sup> fluoride, to ensure the value attained for NaF solution was representative of the fluoride ligand-exchange reaction only, rather than any crystallisation mechanisms. An XRD spectrum of the resin, post-treatment, confirmed no crystalline species were present (Supporting Information, Fig. S38). For both matrices,  $R^2$  values for Arrhenius plots were reasonable. The  $E_a$  value derived for NaF solution uptake is similar to the figure of 68.7 kJ mol<sup>-1</sup> obtained by Na & Park in the uptake of fluoride by La(OH)<sub>3</sub> at a similar  $C_i$  [58]. The lower  $E_a$  value for leachate uptake is nonetheless suggestive of a chemisorption mechanism, since diffusion-controlled processes result in  $E_a$  values of <30 kJ mol<sup>-1</sup> [49, 50]. We propose that the dominant uptake mechanism from leachate is closely related to the depiction in Fig.4, with multi-nuclear complexes formed between P, La and Al centres, with O and F bridging ligands.

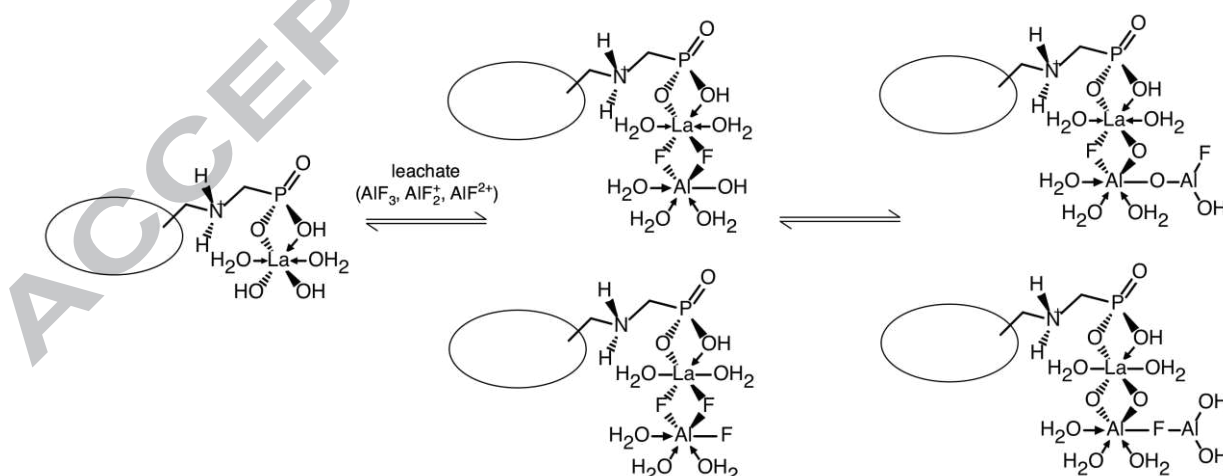


**Fig. 4.** Proposed modified uptake mechanism of fluoride and aluminium from SPL leachate on La-MTS9501. Coordinated waters for secondary AHF complexation are omitted for clarity.

Xu *et al.* have reported a novel La/Al-hydroxide composite material that was spontaneously formed in varying molar ratios in an aqueous environment [62].

Lanthanides are known to partake in multi-nuclear complex formation, with fluoride bridges to first-row transition metals, although complexation with Al has not yet been reported [63]. Lyu *et al.* also investigated modified zeolites for fluoride removal and found that when the material was loaded with both La and Al, a synergistic effect was observed, giving the sorbent a higher capacity than Al or La alone [64]. The lower  $E_a$  values in comparison to simple ligand-exchange may be explained by the chelating effect, which may be favoured in high ionic strength conditions [65, 66]. The modified proposed uptake mechanism is consistent with the lack of crystalline AHF species detected on the resin surface and also the unique La environments previously observed in X-ray photoelectron spectroscopy measurements [30]. TGA traces (Supporting Information, Fig. S39) show a significant difference in the final % mass between pre-treatment and leachate-treated La-MTS9501 samples, which could be attributed to the adsorbed Al species, which would essentially be converted to  $Al_2O_3$ .

### 3.3. Generation of breakthrough profiles from dynamic experiments

Breakthrough curves for the two matrices were attained for an inlet fluoride concentration of 15 and 1500 mg L<sup>-1</sup> and are shown in Figs. 5 and 6. In the case of the as-prepared leachate experiment, the profiles of Al and Ca were also determined and the concentrations of the other common anions in the effluent were also checked, to monitor the behaviour of coexisting ions, relative to the fluoride breakthrough (Fig. 7). Leaching of La was checked, but its concentration in the

eluent was found to be  $<0.1 \text{ mg L}^{-1}$  throughout the experiment. Extracted parameters from the Dose-Response model are presented in Table 3.

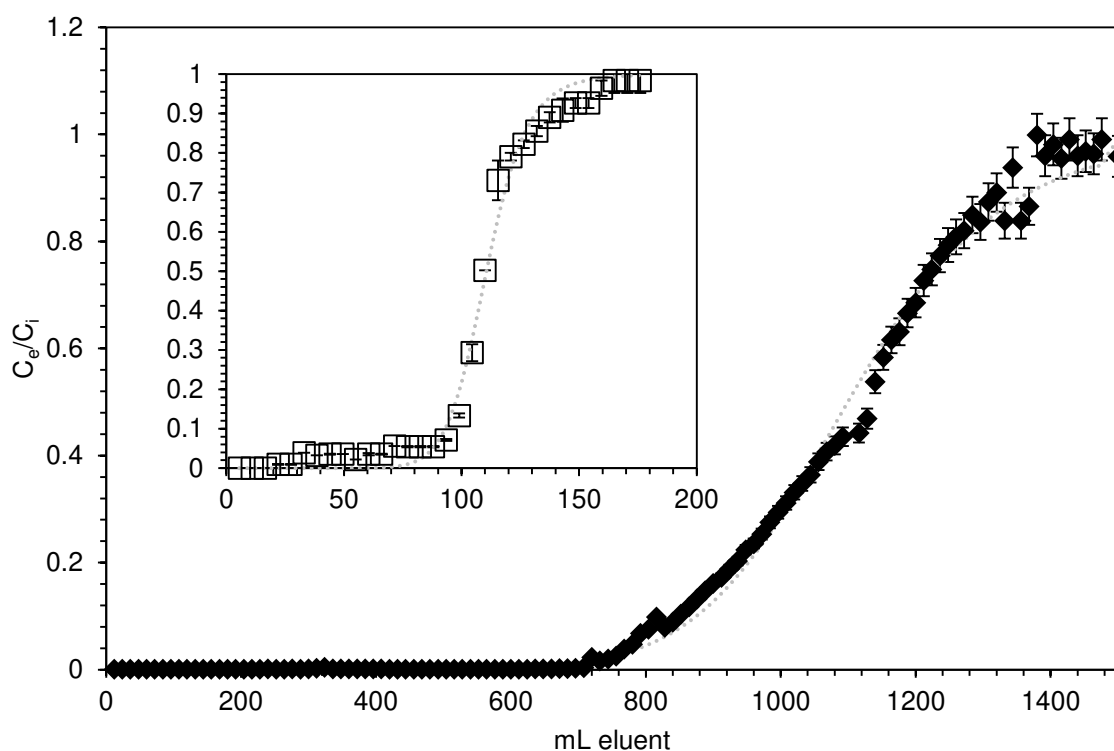


**Fig. 5.** Fluoride breakthrough profile attained by passing 1/100 diluted leachate ( $\blacklozenge$ ) and NaF solution of  $[F] \sim 15 \text{ mg L}^{-1}$  ( $\square$ ) through a La-MTS9501 column. Dotted lines represent Dose-Response model. Resin bed volume = 6.0 mL. Flow rate =  $1 \text{ BV h}^{-1}$ .  $T = 20^\circ\text{C}$ .

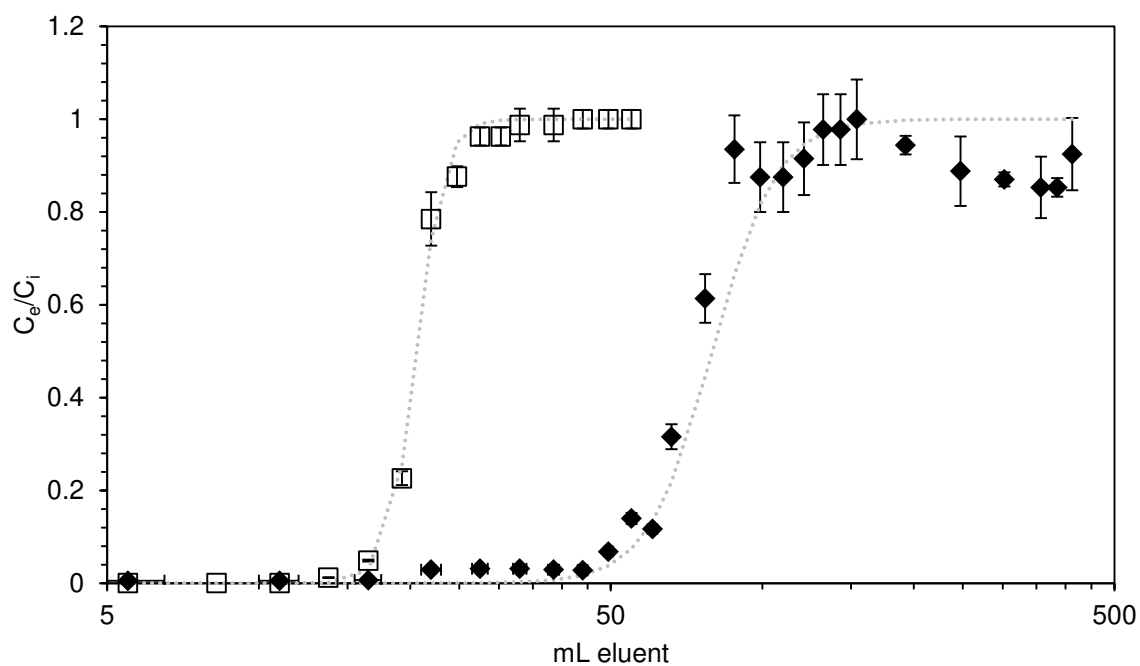


**Fig. 6.** Fluoride breakthrough profile attained by passing as-prepared leachate ( $\blacklozenge$ ) and NaF solution of  $[F] \sim 1500 \text{ mg L}^{-1}$  ( $\square$ ) through a La-MTS9501 column. x axis is logarithmic for clarity. Dotted lines represent Dose-Response model. Resin bed volume = 6.0 mL. Flow rate =  $1 \text{ BV h}^{-1}$ .  $T = 20^\circ\text{C}$ .

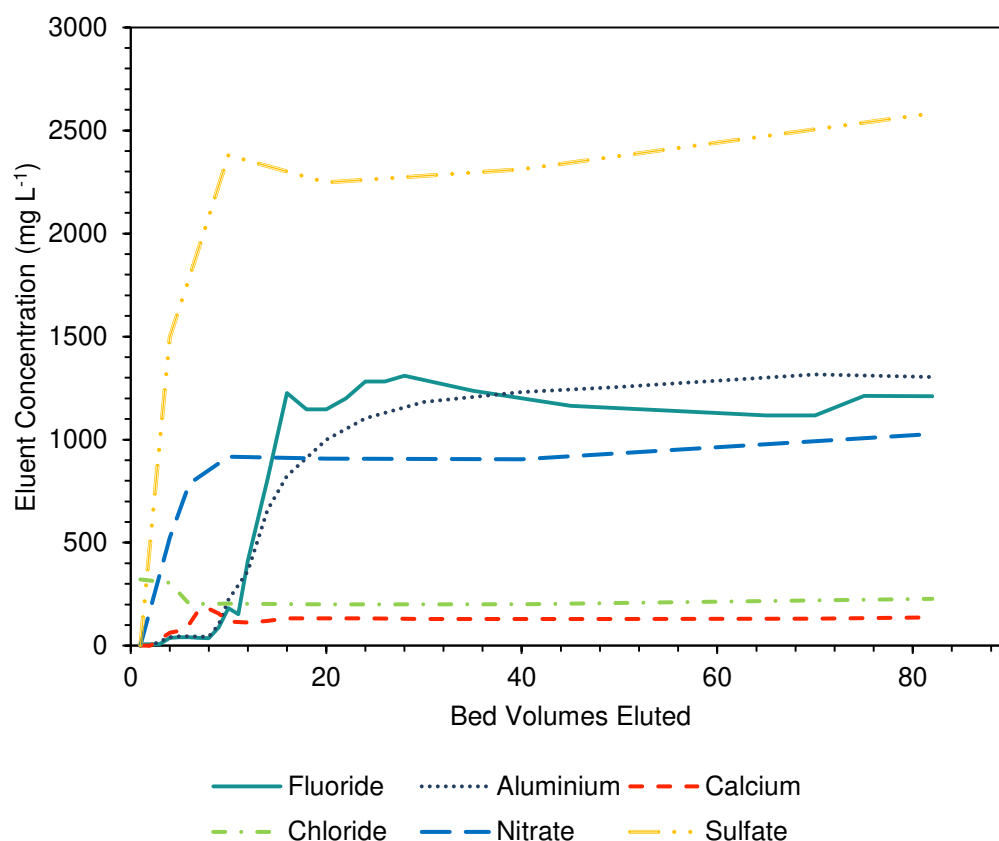


**Fig. 7.** Comparison of co-contaminant concentrations in the effluent during breakthrough experiment with as-prepared leachate. Resin bed volume = 6.0 mL. Flow rate = 1 BV h<sup>-1</sup>. T = 20°C. [Figure to be presented in colour].

**Table 3.** Calculated parameters from Dose-Response model for the systems studied in Figs. 5-9.

Experiment	Dose-Response model parameters			
	<i>a</i>	<i>b</i>	<i>q<sub>0</sub></i> (mg g <sup>-1</sup> )	R <sup>2</sup>
Leachate 1/100 dilution (F)	5.35 ± 0.20	1283 ± 126	4.27 ± 0.42	0.964
Leachate as-prepared (F)	4.43 ± 0.21	79.6 ± 10.9	66.7 ± 9.1	0.955
Leachate as-prepared (Al)	4.78 ± 0.24	77.0 ± 7.5	26.3 ± 01.7	0.995
Leachate as-prepared (Ca)	3.02 ± 0.40	24.0 ± 5.2	1.75 ± 0.38	0.978
NaF solution ([F] ≈ 15 mg L <sup>-1</sup> )	7.36 ± 0.30	116 ± 27	1.15 ± 0.27	0.964
NaF solution ([F] ≈ 1500 mg L <sup>-1</sup> )	16.0 ± 0.8	20.6 ± 2.5	20.5 ± 2.5	0.996

For uptake both from NaF solution and leachate, the Dose-Response model provided the best description of breakthrough behaviour. This model is empirical, so no assumptions about fundamental uptake behaviour can be drawn. However, as is common with other dynamic adsorption studies, the model minimises the errors produced by other models [67-69]. In particular, the Dose-Response equation produced a rather superior fit over a long period of column operation, as the R<sup>2</sup> value

for the dilute leachate experiment (1900 mL eluent) was 0.964 (other models: 0.939 - 0.942). We could not find any previous examples in the literature where this model has successfully been used to describe fluoride breakthrough in a column experiment. Such breakthrough has previously successfully been described by the Thomas model [70], which our results were also in good agreement with, showing an  $R^2$  range of 0.942 – 0.996 (Supporting Information, Table S10). This is predictable, as this model was derived from second-order kinetics, which the sorbent/sorbate interaction was observed to follow in static experiments. From the generally good fits of the Thomas model, it can be concluded that, in a column environment, both free fluoride and AHF adsorption is probably rate-limited not by chemical reaction, but by interfacial mass-transfer [71]. Interestingly, the Thomas kinetic constants ( $k_{Th}$ ) for leachate fluoride-breakthrough were an order of magnitude lower than for NaF solution breakthrough, which again is comparable to static work. The identical agreement of the data with the Yoon-Nelson model (the two being mathematically analogous) indicates that for both matrices, the breakthrough behaviour can be rationalised as the probability of adsorption for each fluoride ion or AHF complex being proportional to probability of adsorption versus probability of breakthrough [47]. The Adams-Bohart model, whilst being limited, in that it cannot describe the full column breakthrough process [71], was also in good agreement with some data, showing an  $R^2$  range of 0.886 – 0.999 (Supporting Information, Table S11). As a result, it is probable that the dynamic adsorption is dependent on both resin residual capacity and fluoride/AHF concentration [67].

In common with static kinetic results,  $q_0$  values, calculated from the Dose-Response model, for the leachate were far larger than for NaF solution (Table 3). This

suggested that an industrial resin column would work efficiently in its intended function and the superiority was observed at both high and low inlet concentration. Interestingly, in the case of as-prepared leachate, fluoride and Al breakthrough occurs within a similar timeframe, as would be expected given the proposed uptake mechanism. However,  $q_0$  values show a higher molar ratio of  $F^-:Al^{3+}$  was taken up in the column study, which is likely because the system does not approach equilibrium, as was the case in static kinetic experiments, so there was not time for the  $F^-/OH^-$  reverse ligand-exchange reaction of the coordinated AHFs to proceed (Fig. 4). The Ca breakthrough curve is dissimilar to Al and fluoride, indicating that  $Ca^{2+}$  ions are not similarly involved in fluoride transfer on to the resin and may instead occupy vacant phosphonic acid coordination sites. Coexisting anions  $NO_3^-$  and  $SO_4^{2-}$  were also observed to breakthrough rapidly, while  $[Cl^-]$  in the effluent exceeded that in the inlet solution for a short period. This behaviour may be due to the N atom in the aminophosphonic acid group acting as an anion-exchange site, since its deprotonation would not readily occur in these experimental conditions [72]. The counter-ion would originally have been  $Cl^-$ , due to the HCl preconditioning of the resin and a certain amount of exchange would be expected, given that  $NO_3^-$  and  $SO_4^{2-}$  are higher in the established anion selectivity series [73].

#### 3.4. Generation of elution profiles from dynamic experiments

The full elution profiles of fluoride, Al and Ca attained from the as-prepared, leachate-loaded La-MTS9501 column are shown in Fig. 8). A number of BVs were also analysed for pH,  $Cl^-$ ,  $NO_3^-$  and  $SO_4^{2-}$  concentrations and the relationships between these and fluoride and cation concentrations are also shown. The

equivalent elution profile for fluoride only, attained from the NaF solution-loaded La-MTS9501 column (fluoride  $C_i \approx 1500 \text{ mg L}^{-1}$ ) is shown in Fig. 9.

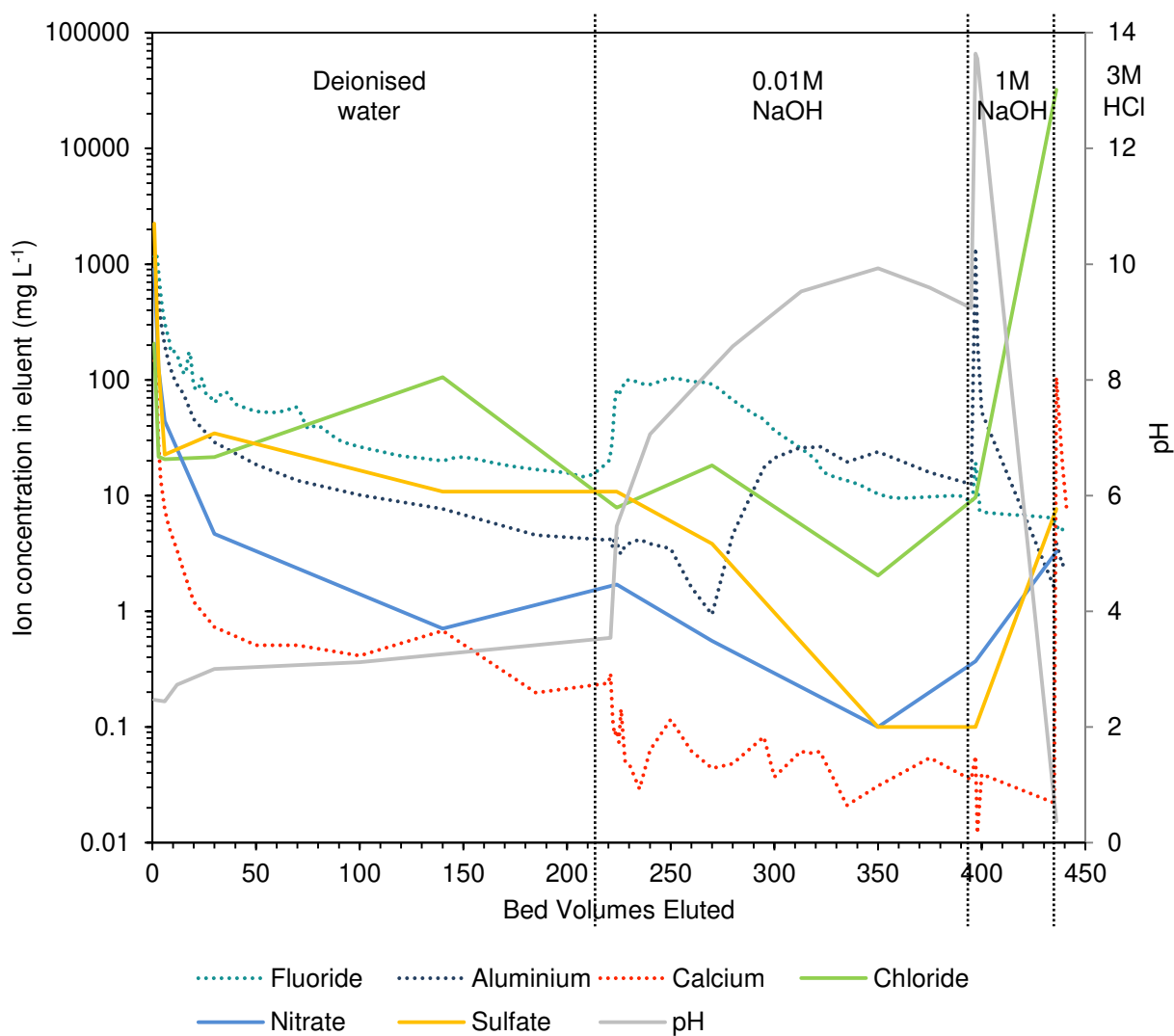


**Fig. 8.** Elution of  $F^-$ ,  $Al$ ,  $Ca$ ,  $Cl^-$ ,  $NO_3^-$  and  $SO_4^{2-}$  from leachate-loaded La-MTS9501 column. Y axis is logarithmic for clarity. Vertical lines indicate change in eluent. Resin bed volume = 6.0 mL. Flow rate =  $1 \text{ BV h}^{-1}$ .  $T = 20^\circ\text{C}$ . [Figure to be presented in colour].

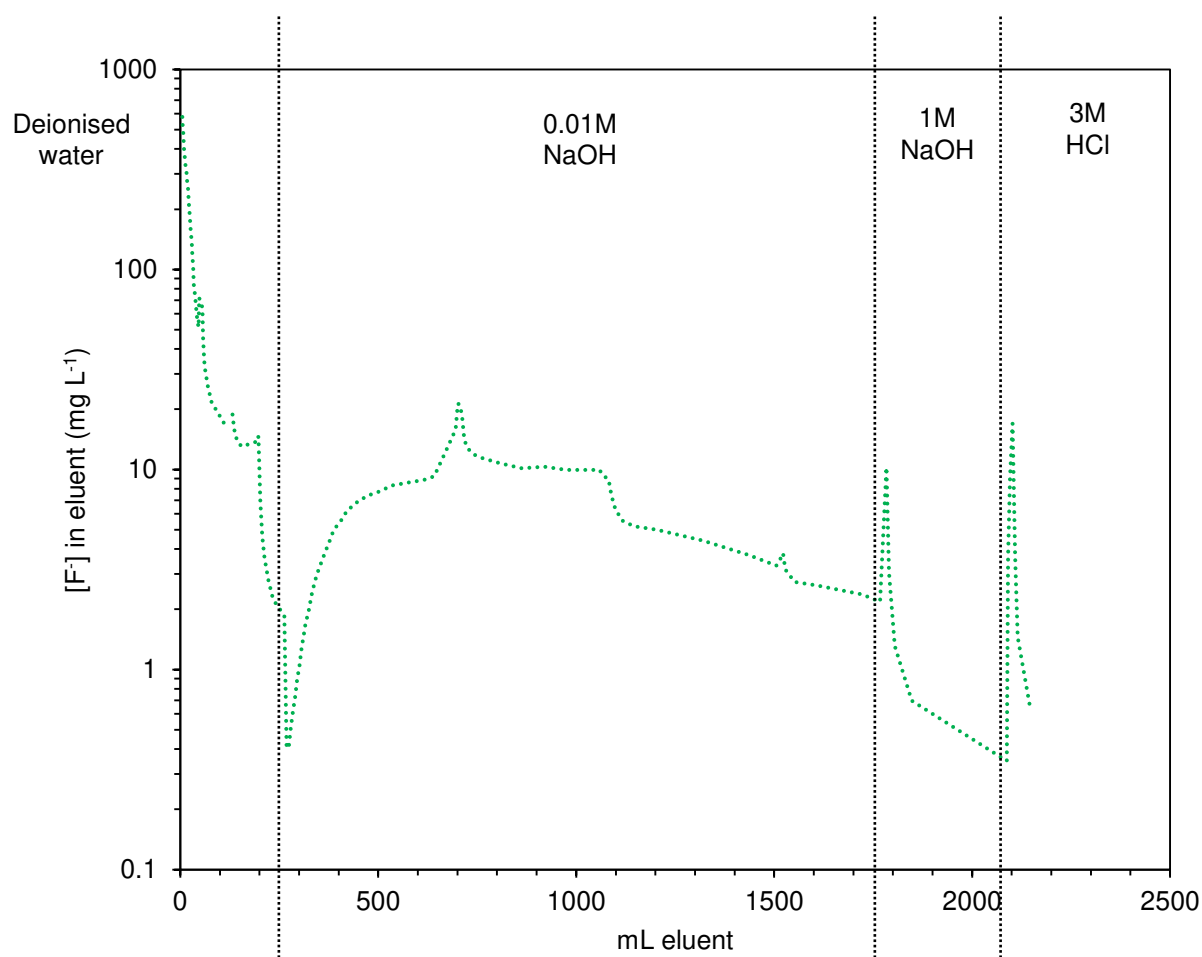


**Fig. 9.** Elution of fluoride from NaF solution-loaded La-MTS9501 column. Y axis is logarithmic for clarity. Vertical lines indicate change in eluent. Resin bed volume = 6.0 mL, flow rate = 1 BV h<sup>-1</sup>. T = 20°C. [Figure to be presented in colour].

Fluoride % recoveries were calculated as  $95.7 \pm 14.1$  % for the leachate-loaded column and  $87.1 \pm 5.3$  % for the NaF-loaded column. Al and Ca % recovery were calculated as  $106 \pm 7$  % and  $109 \pm 12$  % respectively for the leachate-loaded column. This good agreement supports the validity of the Dose-Response model as a tool for predicting breakthrough behaviour for all three species.

Literature sources have reported that metal-loaded resins may be regenerated for fluoride uptake by dilute NaOH treatment [53, 74]. In this instance, for the NaF-loaded column (Fig. 9), a significant amount of fluoride remained on the resin after

the 0.01 M NaOH eluent stage and was only eluted by 1 M NaOH or even remained bound until the La-loading was removed by 3 M HCl. The majority of fluoride eluted very rapidly with deionised water as the eluent, which is likely to represent the weakly-physisorbed crystalline NaF, with elution essentially caused by the change in concentration gradient. The latter stages of the elution suggest a variety of binding sites of different strengths are present on the resin. This is consistent with previous Freundlich isotherm data, which indicated that the resin surface was heterogeneous in energy [30]. The stronger sites may be attributed to fluoride ligands which bridge between two adjacent La centres [63]. The elution peak caused by 0.01 M NaOH is broad and shallow, suggesting that relatively concentrated NaOH may be a better choice for elution of concentrated, pure fluoride aqueous streams, for  $\text{CaF}_2$  precipitation and recovery, since an inlet  $[\text{F}^-] > 100 \text{ mg L}^{-1}$  is required for such a process [75]. The peak is also poorly resolved and suggests a number of micro-environments, of slightly different binding energy were present. This agrees with the heterogeneity of the adsorption, proposed in our previous work [30].

The leachate-loaded column (Fig. 8) exhibited co-elution of fluoride and Al with deionised water as the eluent. Significant fractions of both species were also eluted with NaOH. This again indicates a range of different strength binding sites.

Interestingly, although the fluoride effluent concentration increases upon changing the eluent to 0.01 M NaOH, the Al effluent concentration actually falls significantly. This may be explained by a reverse ligand-exchange process, in which  $-\text{F}$  is replaced by  $-\text{OH}$ , without dissociation of the proposed binuclear coordinated complexes. The Al then appears to slowly begin to dissociate from the resin surface, before being completely removed by the change to 1 M NaOH. The eluent pH over

this timeframe increases from ~6–10 and, as reported by Lisbona and Steel [27], the anionic species  $[\text{AlF}_3(\text{OH})]^-$  and  $[\text{AlF}_2(\text{OH})_2]^-$  gradually become dominant over this range in  $\text{F}^-/\text{Al}$  systems as pH increases. The behaviour is hence explained, as these species would be exchanged with  $\text{OH}^-$  ions on the La coordination sites and subsequently elute. The probable changes to the functional group chemistry throughout the elution process are postulated in Fig. 10.

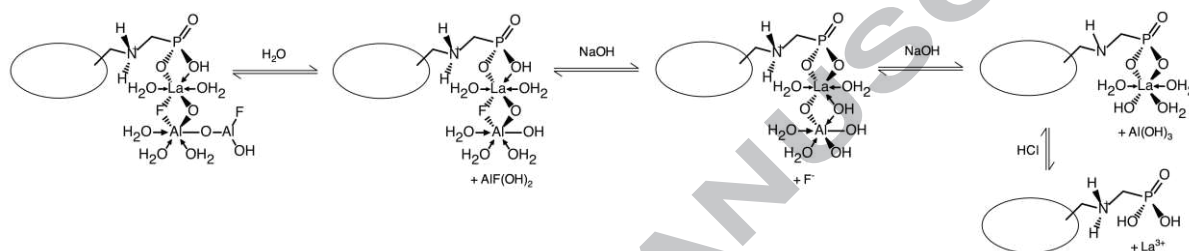


**Fig. 10.** Proposed desorption processes from leachate-loaded La-MTS9501 column with changing eluent.

As seen in Fig. 8, the pH of the effluent did not rise above 10 until after the eluent change to 1 M NaOH. Hence it can be assumed that the functional group N atoms were not deprotonated until this point and the observed elution of  $\text{Cl}^-$ ,  $\text{NO}_3^-$  and  $\text{SO}_4^{2-}$  in the early stages of the experiment was likely due to weak electrostatic interaction of the anions with a positively charged resin surface during loading [48].

### 3.5. Performance of the resin over repeated equilibrium batch cycles

The variations in approximate maximum uptake capacity of the resin over five cycles of regeneration with 0.01 M NaOH is shown in the Supporting Information, Fig. S36.

The performance of the resin was actually increased slightly, on average, over the sequence of regenerations. We may attribute this to the lesser amount of  $\text{Cl}^-$  ions electrostatically associated with the resin surface. The concentration would be substantial during cycle 1 (directly after loading with  $\text{La}^{3+}$  as  $\text{LaCl}_3 \cdot 7\text{H}_2\text{O}$ ). Whilst acting only as an outer-sphere ligand, [76] the presence of  $\text{Cl}^-$  may cause a slight

barrier to the La/AHF complexation reaction, which is removed with the NaOH treatment. The results demonstrate the feasibility of use of NaOH as the eluting agent for fluoride commodity chemicals recovery. A further advantage practically, is that the resin could be put straight back into operation, after washing with water, as the high ionic strength liquor naturally buffers the pH towards favourable fluoride uptake conditions [30]. The success of the complete regeneration with acid indicates that the resin could be restored to full effectiveness in the event of any long-term degradation caused by many cycles of NaOH treatment.

### 3.6. Effect of $\text{Al}^{3+}$ on resin performance in equilibrium batch studies

The effect of the ratio of  $\text{F}^-:\text{Al}^{3+}$  in the leachate on fluoride uptake in batch experiments is shown in the Supporting Information, Fig. S37. The ratio of  $\text{F}^-:\text{Al}^{3+}$  is strongly influential to resin performance with the mass ratio of 1.5:1  $\text{F}^-:\text{Al}^{3+}$  being very beneficial to fluoride transfer, which is obviously close to the ratio within the SPL leachate. Conversely, both very low and very high  $[\text{Al}^{3+}]$  suppressed the fluoride uptake. The former may be explained by the presence of  $\text{NO}_3^-$  and  $\text{SO}_4^{2-}$ , which, as O-donors, may compete for La centre coordination sites with free fluoride, according to concentration gradient laws [77]. The latter is likely because at high  $[\text{Al}^{3+}]$ , the dominant aqueous Al species will be  $\text{Al}(\text{OH})_3$  (Supporting Information, Table S4) [32], which may interact with the aminophosphonic acid group in the same manner as  $\text{AlF}_2^+$  and  $\text{AlF}_3$ . Hence minimal fluoride uptake occurs. Indeed, ICP measurements of the  $500 \text{ mg L}^{-1} \text{ Al}^{3+}$  sample solution indicated an Al  $q_e$  of  $32.4 \text{ mg g}^{-1}$ , whereas fluoride uptake was negligible.

The  $F^-:Al^{3+}$  ratio is clearly of concern from an applied perspective, as the composition of SPL and hence the derived leachate is variable, depending on smelter type and cell decommissioning process [7]. The ratio could however, be monitored by in-situ analysis of the leachate feedstock by fluoride ISE, since  $[Al^{3+}]$  can be simultaneously determined [78]. The ratio may be altered by addition of Al salts. Also, primary Al production results in gaseous HF formation, which is captured by a caustic scrubbing solution. This stream could also be used for control of the ratio.

### 3.7. Pathways to recovery of commodity products from the eluent

A desirable recovery product from SPL leaching would be the  $AlF_3$  precursor  $AlF_2OH \cdot H_2O$ , which may be reacted with gibbsite ( $Al(OH)_3$ ) and anhydrous HF to produce the desired product. However, the precipitation of  $AlF_2OH \cdot H_2O$  has been shown to require a specific  $F^-:Al$  ratio of 1.6:1 and must be achieved starting with a concentrated acidic initial solution, followed by careful raising of the pH, to avoid undesirable co-precipitation of sodium-containing species [79]. The resulting  $[F^-]$  and  $[Al^{3+}]$  achieved in Fig. 8 with deionised water as the eluent would not be sufficient and an evaporation step would be required. Elution with deionised water, followed by strong acid is an option, but would lead to complete loss of La from the resin. The most feasible recovery strategy would be as follows: The column would be first eluted with deionised water, to eject the undesirable Ca and anions. As seen in Fig. 8, the eluent produced here is still fluoride-rich and could be partially recycled back into the lead ion-exchange column after a secondary desalination treatment with a strong-base anion resin column, hence conserving the fluoride in this fraction. The eluent would then change to 1 M NaOH, which would produce a concentrated and pure aqueous stream of  $Na^+$ ,  $F^-$  and  $Al^{3+}$ . Synthetic cryolite could then be readily

precipitated from this solution by lowering the pH [16, 80]. The total masses of fluoride and Al eluted during the NaOH eluent stage were 49.2 and 26.2 mg respectively (Fig. 8). This equates to an approximate  $F^-:Al^{3+}$  molar ratio of  $\sim 2.5:1$ , which is feasible for cryolite precipitation [79]. Although not as valuable as  $AlF_3$ , cryolite is nonetheless a desirable commodity for Al smelting and indeed other uses outside the industry [80]. Unlike  $AlF_3$ , it does not require a calcination step after precipitation, merely requiring drying at  $\sim 40^\circ C$  [10]. Al smelters have historically captured waste fluoride from the Hall-Heroult process as HF by caustic scrubbers and cryolite is attained from this feed by addition of  $Al_2(SO_4)_3$  [81]. The advantage of our proposed process (aside from the effective treatment of SPL and recycling of the additional fluoride reserves within the material) is that there would already be a source of Al in the feed. The purity of the material would also likely exceed current industrial grades.

#### 4. Conclusions

We have investigated the kinetic and dynamic behaviour of fluoride uptake by a novel, Lanthanum-loaded aminophosphonic acid chelating resin La-MTS9501, with a view to instigating an ion-exchange treatment for the recovery of fluoride commodity products from spent potlining leachate. In kinetic tests, fluoride removal from

simulant leachate was considerably greater than from NaF solutions, but uptake rate constants were slower by an order of magnitude. Both systems however, could be described by pseudo second-order kinetics. Activation energies for the uptake processes were calculated and indicated that the uptake mechanism for the leachate was a much lower energy process. This may be explained by a novel chelation interaction between resin-bound La centres and aqueous  $\text{AlF}^{2+}$ ,  $\text{AlF}_2^+$ , and  $\text{AlF}_3$  complexes, forming multi-nuclear coordination species and leading to the enhanced uptake.

In dynamic studies La-MTS9501 again demonstrated a large loading capacity, with breakthrough behaviour well-described by the Dose-Response model. This supports previous work in concluding that solutions of high initial fluoride concentration may be treated efficiently by an ion-exchange column process. Stripping behaviour for both matrices was unusual, with the loaded fluoride eluting over a number of stages with changes to the eluent. The NaF-loaded column profile was dominated by slow elution of crystallised NaF, while the leachate-loaded column profile suggested first, desorption of weakly-bound AHFs, followed by a reverse  $\text{F}^-/\text{OH}^-$  ligand-exchange process and finally dissociation of the La/AHF complexes. By studying the co-elution of contaminants and pH of the eluent, it was concluded that synthetic cryolite was a feasible recovery product for the process. Puromet<sup>TM</sup> MTS9501 is an economical sorbent, available in industrial quantities for  $\sim\text{£}12 \text{ L}^{-1}$  and was shown in this study to perform robustly over 5 loading/stripping cycles. It is hoped that this work will contribute towards development of an optimum hydrometallurgical treatment system for spent potlining and thus contribute to preservation of global fluorspar reserves.

## Note

We refer throughout this article to the commercial resin used as “Puromet™ MTS9501”. Our previous work, using the same resin refers to the material as “Purolite® S950+”, which was its original commercial title.

## Declarations of interest

None.

## Acknowledgements

The authors thank all members of the SNUCER group, University of Sheffield, for their support of this work; in particular Dr Sarah Pepper, for ICP-OES analysis. Thanks to Mr Rob Hanson (Department of Chemistry, University of Sheffield), for TGA training. Thanks to Mr Duncan Schofield and Mr Keith Penny (Department of Chemical and Biological Engineering, University of Sheffield) for IC training. We also gratefully acknowledge Purolite® for their donation of the MTS9501 resin.

## Funding

This work was supported by the EPSRC (Grant no. EP/L016281/1) and Bawtry Carbon International Ltd.

## 6. References

- [1] European Commission, Communication from The Commission to The European Parliament, The Council, The European Economic and Social Committee and The Committee of The Regions. On the 2017 list of Critical Raw Materials for the EU, European Union, Brussels (2017).
- [2] A. Dreveton, Manufacture of high-bulk density aluminium fluoride from fluosilicic acid (HBD-AlF<sub>3</sub> from FSA) and AHF, First Symposium on Innovation and Technology in the Phosphate Industry, Marrakech (2011).
- [3] V. Davis, C. Bates, B. Savoie, Q. Xu, W. Wolf, M. Webb, K. Billings, R. Mckenney, I. Darolles, N. Nair, A. Hightower, D. Rosenberg, A. Musahid, C. Brooks, T. Miller, R. Grubbs, S. Jones, Science, 362 (2018) 1144-1148.

- [4] T. Kameda, J. Oba, T. Yoshioka, *Journal of Hazardous Materials*, 300 (2015) 475-482.
- [5] A. Ezzeddine, A. Bedoui, A. Hannachi, N. Bensalah, *Desalination and Water Treatment*, 54 (2015) 2280-2292.
- [6] M. Dessalegne, F. Zewge, N. Pfenninger, C.A. Johnson, I. Diaz, *Water Air and Soil Pollution*, 227 (2016) 13.
- [7] G. Holywell, R. Breault, *Journal of The Minerals, Metals and Materials Society*, 65 (2013) 1441-1451.
- [8] M. Iffert, PhD thesis, The University of New South Wales, Sydney, Australia (2007).
- [9] H. Kvande, in *Production of Primary Aluminium*, R. Lumley Ed., Woodhead Books, Sawston, Cambridge (2011).
- [10] K. Jiang, K. Zhou, *Euro-Mediterranean Journal for Environmental Integration*, 2 (2017) 22.
- [11] Roskill, *Fluorspar. Global Industry, Markets and Outlook 2018*, Roskill Information Services, Wimbledon (2018).
- [12] W. Li, X. Chen, Running results of the SPL detoxifying pilot plant in Chalco, Light Metals, Aluminium Reduction Technology, Cell Development and Operations - Part 1, Auckland, New Zealand (2006).
- [13] T. Hopkins, P. Merline, *Mineral Processing and Extractive Metallurgy Review*, 15 (1995) 247-255.
- [14] P. Black, B. Cooper, A Natural "Industrial Ecology" Based Solution for Spent Potlining: Closing the loop for aluminium in the circular economy, R. Services Ed., Victoria, Australia (2015).
- [15] L. Birry, S. Leclerc, S. Poirier, *TMS (The Minerals, Metals & Materials Society), Light Metals* (2016) 467-471.
- [16] Z.-N. Shi, W. Li, X.-W. Hu, B.-J. Ren, B.-L. Gao, Z.-W. Wang, *Transactions of the Nonferrous Metals Society of China*, 22 (2012) 222-227.
- [17] R. Breault, S.P. Poirier, G. Hamel, A. Pucci, in A 'green' way to deal with spent pot lining, *Aluminium International Today* (2011).
- [18] K. Oke, S. Neumann, B. Adams, *Water Today*, May (2011) 76-80.
- [19] N. Viswanathan, S. Meenakshi, *Journal of Fluorine Chemistry*, 129 (2008) 645-653.
- [20] F. Luo, K. Inoue, *Solvent Extraction and Ion Exchange*, 22 (2004) 305-322.
- [21] S.M. Prabhu, S. Meenakshi, *Desalination and Water Treatment*, 52 (2014) 2527-2536.
- [22] J.M. Cheng, X.G. Meng, C.Y. Jing, J.M. Hao, *Journal of Hazardous Materials*, 278 (2014) 343-349.
- [23] S.A. Wasay, S. Tokunaga, S.-W. Park, *Separation Science and Technology*, 31 (1996) 1501-1514.
- [24] P. Liang, Y. Zhang, D.F. Wang, Y. Xu, L. Luo, *Journal of Rare Earths*, 31 (2013) 817-822.
- [25] E. Kusriani, N. Sofyan, N. Suwartha, G. Yesya, C.R. Priadi, *Journal of Rare Earths*, 33 (2015) 1104-1113.
- [26] S. Meenakshi, N. Viswanathan, *Journal of Colloid and Interface Science*, 308 (2007) 438-450.
- [27] D.F. Lisboa, K.A. Steel, *Separation and Purification Technology*, 61 (2008) 182-192.
- [28] G.J. Millar, S.J. Couperthwaite, D.B. Wellner, D.C. Macfarlane, S.A. Dalzell, *Journal of Water Process Engineering*, 20 (2017) 113-122.

- [29] K.M. Popat, P.S. Anand, B.D. Dasare, *Reactive Polymers*, 23 (1994) 24-32.
- [30] T. Robshaw, S. Tukra, D.B. Hammond, G.J. Leggett, M.D. Ogden, *Journal of Hazardous Materials*, 361 (2019) 200-209.
- [31] M.M. Hyland, E.C. Patterson, F. Stevens-McFadden, B.J. Welch, *Scandinavian Journal of Metallurgy*, 30 (2001) 404-414.
- [32] H. Kalka, *Aqion Manual (selected topics)* [online], <http://www.aqion.de/site/98?>, (2015).
- [33] V.Y. Bazhin, R.K. Patrin, *Refractories and Industrial Ceramics*, 52 (2011) 63-65.
- [34] T.K. Pong, R.J. Adrien, J. Besida, T.A. O'Donnell, D.G. Wood, *Process Safety and Environmental Protection*, 78 (2000) 204-208.
- [35] S. Lagergren, *Svenska Vetenskapsakademiens. Handlingar*, 24 (1898) 1-39.
- [36] G. Blanchard, M. Maunaye, G. Martin, *Water Research*, 18 (1984) 1501-1507.
- [37] G.E. Boyd, A.W. Adamson, L.S. Myers Jr., *Journal of The American Chemical Society*, 69 (1947) 2836-2848.
- [38] N.T.T. Tu, T.V. Thien, P.D. Du, V.T.T. Chau, T.X. Mau, D.Q. Khieu, *Journal of Environmental Chemical Engineering*, 6 (2018) 2269-2280.
- [39] W.J. Weber, J.C. Morris, *Journal of the Sanitary Engineering Division*, 89 (1963) 31-60.
- [40] S.E. Pepper, K.R. Whittle, L.M. Harwood, J. Cowell, T.S. Lee, M.D. Ogden, *Separation Science and Technology*, 53 (2018) 1552-1562.
- [41] H.N. Tran, S.J. You, A. Hosseini-Bandegharai, H.P. Chao, *Water Research*, 120 (2017) 88-116.
- [42] S. Roginsky, Y.B. Zeldovich, *Acta Physicochimica U.R.S.S.*, 1 (1934) 554.
- [43] S.H. Chien, W.R. Clayton, *Soil Science Society of America Journal*, 44 (1980) 265-268.
- [44] G.Y. Yan, T. Viraraghavan, M. Chen, *Adsorption Science & Technology*, 19 (2001) 25-43.
- [45] J.P. Bezzina, M.D. Ogden, E.M. Moon, K.L. Soldenhoff, *Journal of Industrial and Engineering Chemistry*, 59 (2018) 440-455.
- [46] L. Lv, J. He, M. Wei, X. Duan, *Industrial & Engineering Chemistry Research*, 45 (2006) 8623-8628.
- [47] E.B. Simsek, U. Beker, B.F. Senkal, *Desalination*, 349 (2014) 39-50.
- [48] Y. Ku, H.M. Chiou, H.W. Chen, *Journal of the Chinese Institute of Engineers*, 34 (2011) 801-807.
- [49] L. Fang, K.N. Ghimire, M. Kuriyama, K. Inoue, K. Makino, *Journal of Chemical Technology and Biotechnology*, 78 (2003) 1038-1047.
- [50] A.J. Canner, S.E. Pepper, M. Hayer, M.D. Ogden, *Progress in Nuclear Energy*, 104 (2018) 271-279.
- [51] L.M. Camacho, A. Torres, D. Saha, S.G. Deng, *Journal of Colloid and Interface Science*, 349 (2010) 307-313.
- [52] E. Vences-Alvarez, L.H. Velazquez-Jimenez, L.F. Chazaro-Ruiz, P.E. Diaz-Flores, J.R. Rangel-Mendez, *Journal of Colloid And Interface Science*, 455 (2015) 194-202.
- [53] M.J. Haron, W.M.Z. Yunus, *Journal of Environmental Science and Health Part a-Toxic/Hazardous Substances & Environmental Engineering*, 36 (2001) 727-734.
- [54] D.B. Bhatt, P.R. Bhatt, H.H. Prasad, K.M. Popat, P.S. Anand, *Indian Journal of Chemical Technology*, 11 (2004) 299-303.
- [55] Lanxess, *Product Information: Lewatit TP260*, [online] <https://www.lenntech.com/Data-sheets/Lewatit-TP-260-L.pdf> (2011).

- [56] Purolite, in Product data sheet. Puromet MTS9501, [online] <https://www.purolite.com/product-pdf/MTS9501.pdf> (2018).
- [57] M.J. Moreira, L.M. Ferreira, *Journal of Chromatography A*, 1092 (2005) 101-106.
- [58] C.K. Na, H.J. Park, *Journal of Hazardous Materials*, 183 (2010) 512-520.
- [59] Y. Liu, L. Shen, *Langmuir*, 24 (2008) 11625-11630.
- [60] N. Viswanathan, S. Meenakshi, *Journal of Hazardous Materials*, 178 (2010) 226-232.
- [61] N. Viswanathan, S. Meenakshi, *Journal of Hazardous Materials*, 162 (2009) 920-930.
- [62] R. Xu, M.Y. Zhang, R.J.G. Mortimer, G. Pan, *Environmental Science & Technology*, 51 (2017) 3418-3425.
- [63] T. Birk, K.S. Pedersen, C.A. Thuesen, T. Weyhermuller, M. Schau-Magnussen, S. Piligkos, H. Weihe, S. Mossin, M. Evangelisti, J. Bendix, *Inorganic Chemistry*, 51 (2012) 5435-5443.
- [64] Y. Lyu, X.S. Su, S.Y. Zhang, Y.L. Zhang, *Water Air and Soil Pollution*, 227 (2016) 1-9.
- [65] J.L. Sides, C.T. Kenner, *Analytical Chemistry*, 38 (1966) 707-711.
- [66] J.T.M. Amphlett, C.A. Sharrad, M.D. Ogden, *Chemical Engineering Journal*, 342 (2018) 133-141.
- [67] H. Tavakoli, H. Sepehrian, F. Semnani, M. Samadfam, *Annals of Nuclear Energy*, 54 (2013) 149-153.
- [68] B. Zhao, Y. Shang, W. Xiao, C. Dou, R. Han, *Journal of Environmental Chemical Engineering*, 2 (2014) 40-45.
- [69] J.T.M. Amphlett, C.A. Sharrad, R.I. Foster, M.D. Ogden, *Journal of the Southern African Institute of Mining and Metallurgy*, 118 (2018) 1521-1527.
- [70] Y.X. Ma, F.M. Shi, X.L. Zheng, J. Ma, C.J. Gao, *Journal of Hazardous Materials*, 185 (2011) 1073-1080.
- [71] M.H. Calero, F. Blázquez, G. Tenorio, G. Martín-Lara, M.A., *Journal of Hazardous Materials*, 171 (2009) 886-893.
- [72] D. Villemin, M.A. Didi, *Oriental Journal of Chemistry*, 31 (2015) 1-12.
- [73] F.G. Helfferich, *Ion Exchange*, McGraw-Hill, New York (1962).
- [74] M. Kanosato, T. Yokoyama, T.M. Suzuki, *Chemistry Letters*, (1988) 207-210.
- [75] R. Aldaco, A. Garea, A. Irabien, *Water Research*, 41 (2007) 810-818.
- [76] V.S. Sastri, J.-C. Bunzli, V. Ramachandra Rao, G.V.S. Rayudu, J.R. Perumareddi, *Modern Aspects of Rare Earths and their Complexes*, Elsevier, Amsterdam (2003).
- [77] J. Knoeck, *Analytical Chemistry*, 41 (1969) 2069-2071.
- [78] T.J. Hanson, K.M. Smetana, *Determination of Aluminium by Four Analytical Methods*, Atlantic Richfield Hanford Company, Richland, Washington (1975).
- [79] U. Ntuk, S. Tait, E.T. White, K.M. Steel, *Hydrometallurgy*, 155 (2015) 79-87.
- [80] Y. Li, H. Zhang, Z.Q. Zhang, L.M. Shao, P.J. He, *Journal of Environmental Sciences*, 31 (2015) 21-29.
- [81] M.A. Ford, J.d.B. Cunliff, *Hydrometallurgy*, 16 (1986) 283-299.

**Towards the implementation of an ion-exchange system for recovery of fluoride commodity chemicals. Kinetic and dynamic studies**

## Research Highlights

- \* Kinetics of fluoride uptake from spent potlining simulant leachate are demonstrated.
- \* Activation energy for fluoride adsorption via metal-loaded resin is reported.
- \* Resin-bound La ions may chelate with aqueous aluminium hydroxyfluorides.
- \* Column performance is well-described by Dose-Response model.
- \* From elution data, recovery of synthetic cryolite is targeted.

## Towards the implementation of an ion-exchange system for recovery of fluoride commodity chemicals. Kinetic and dynamic studies

### Graphical abstract

